Desalination and Water Treatment
www.deswater.com

(2017) 1–10

doi: 10.5004/dwt.2017.20572

Effective adsorption of methylene blue dye using activated carbon developed from the rosemary plant: isotherms and kinetic studies

M.T. Amin[a,b,*], A.A. Alazba[a,c], M. Shafiq[a]

[a]*Alamoudi Water Research Chair, King Saud University, P. O. Box 2460, Riyadh 11451, Saudi Arabia, Tel. +966114673737; Fax: +966114673739, email: mtamin@ksu.edu.sa (M.T. Amin)*
[b]*Department of Environmental Sciences, COMSATS Institute of Information Technology, Abbottabad 22060, Pakistan*
[c]*Agricultural Engineering Department, King Saud University, P. O. Box 2460, Riyadh 11451, Saudi Arabia*

Received 28 June 2016; Accepted 10 February 2017

ABSTRACT

In this study, the adsorption efficiency of the inactivated rosemary (RM) plant and the derived activated carbon (RMAC) for the removal of methylene blue (MB) dye were investigated. RM and RMAC displayed maximum adsorption capacities of 153.17 and 110.67 mg g^{-1}, respectively, for optimum batch conditions. The MB adsorption data of both RM and RMAC were better described by the Langmuir isotherm model than the Freundlich isotherm models; however, the former showed the physical adsorption with a mean free energy of 8.08 kJ mol^{-1} and the latter reflected the chemisorption with mean free energy of 28.87 kJ mol^{-1}. The MB adsorption of both adsorbents followed the pseudo-second-order kinetics model. The MB dye adsorption process was determined to be a non-spontaneous and exothermic reaction for the RM adsorbent, whereas the RMAC reflected the spontaneous and endothermic nature of the MB adsorption. This study showed that the RMAC can be used as an efficient sorbent for MB dye removal in comparison with its non-activated form.

Keywords: Activated carbon; Adsorption; Isotherm models; Methylene blue; Rosemary plant

1. Introduction

Untreated effluents from the textile industry are posing a serious threat to the sustainability of aquatic ecosystems as well as to human health. Methylene blue (MB), a cationic dye, is frequently used in the textile sector, for dying cotton, wool, silk and acrylic dying [1,2]. This dye has been reported to impair the photosynthetic activity in plants. Moreover, it causes skin irritation, cancer, diarrhoea, eye burn as well as, mutagenicity in animals [3]. Therefore, looking at these hazardous effects, it is imperative to treat MB dye from textile effluents before dumping it into freshwater ecosystems.

Different conventional physical and chemical methods are used for the treatment of coloured wastewater. Various physiochemical methods, such as reverse osmosis, sedimentation, ultrafiltration, solvent extraction, electrochemical adsorption, catalysis, coagulation, ion exchange, electrolysis and photo-oxidation are extensively used for the study of textile wastewater treatment [4–7]. Among these technologies commonly used for decolourization of textile wastewater, the adsorption has been shown as efficient due to its friendly operation, design simplicity and insensitivity to toxicity [8]. Conventional adsorbents include commercially activated carbon (AC), chemically modified AC and AC prepared physically from pyrolysis. Plant wastes composed of celluloses and lignin materials could be another alternate choice due to their abundance and low-cost source for AC preparation [9]. These types of wastes possess low concentration of inorganic materials, as these materials affect the adsorption capacity of the activated adsorbent. Moreover, volatile contents above 50%, facilitate the creation of porosity [10].

Rosemary (RM) plant is relatively drought tolerant. It is used in landscaping as a hedge plant and grown in rock gardening, especially during spring. When spring is over, this hedge is either burnt or thrown away, which is

* Corresponding author.

one reason for using this plant as a waste resource for the removal of contaminant in its unmodified form and for the subsequent preparation of AC. This plant has some useful chemical compounds including rosmarinic acid, bornyl acetate, caffeic acid, limonene, rosmaridiphenol, rosmanol and camphor. RM plant leaves has some proportion of lignocellulosic materials like lignin, cellulose, hemicellulose and pectin [11,12]. For this reason, a lignocellulosic material is preferred as adsorbent for adsorption technique as is the case in the current study. The literature suggests that this plant has been used in phytoextraction or rhizofiltration of azo dyes [13,14]. The oil of this plant is used in the synthesis of multi-walled carbon nanotubes, which have been synthesized by a simple spray pyrolysis method using the *Rosmarinus officinalis* oil on an Fe/Mo catalyst supported on silica [15]. The carbonized *R. officinalis* leaves have been used for removal of Hg(II) from aqueous solution [16]. However, to the best of our knowledge, AC is prepared from a non-conventional precursor, i.e., a whole *R. officinalis* plant for the first time and is then subsequently used as an adsorbent for textile dye removal [17–19].

AC synthesis from organic materials consists of two steps: the first step is the carbonization; which increases the carbon content as well as helps in the production of initial porosity. The second step involves the activation of precarbonized materials, which increases the total porosity. In physical activation, carbonization is carried out in the presence of nitrogen gas (an inert atmosphere), followed by oxidization (using carbon dioxide). However, in chemical activation, the precursor is impregnated with chemicals such as H_3PO_4, $ZnCl_2$, $AlCl_3$, NaOH or KOH and then carbonized [20]. Furthermore, chemical activation is preferred over physical because it creates mesoporosity in the adsorbent [18]. Therefore, continuous efforts are being made in exploring waste adsorbents and producing AC from these waste precursors for dye and metal removal for which they show high efficiency [21–23].

In this study, RM, *R. officinalis* was explored in its inactivated form (denoted as RM) and activated carbon (AC) form (denoted as RMAC) for MB dye removal potential under the batch adsorption system. The influence of the process parameters was investigated and these parameters included the agitation speed, contact time, pH, initial dye concentrations and temperature. The mechanisms and adsorptive nature of the RM and RMAC were studied using several isotherms and kinetic models, whereas the spontaneity of the reaction was assessed through a thermodynamic study.

2. Materials and methods

2.1. Preparation of adsorbent and reagent

Waste biomass of RM plant, i.e., branches, leaves and roots (whole plant) were collected from different locations in Riyadh, Kingdom of Saudi Arabia. This plant is relatively drought tolerant and is used in landscaping as a hedge plant and grown in rock gardening especially during spring. When spring is over, this hedge is either burnt or thrown away, which is one reason for using this plant as a waste resource for the removal of contaminant in its unmodified form and for the subsequent preparation of AC. The biomass was washed to remove any adhered soil particles using deionized water. Then, it was dried, ground and sieved and stored in air tight containers. MB dye (C.I. 52015, Merck, Germany) was used as a reagent. A stock solution of MB 1,000 mg L^{-1} was prepared by dissolving 1 g of dye in 1,000 mL deionized water. The working solutions of the required concentrations were prepared by diluting them with deionized water. The absorbance measurements were taken on a UV–Vis spectrophotometer (PG 80^+, UK) using a maximum wavelength of 668 nm.

2.2. Synthesis of activated carbon from rosemary plant waste

The conditions of AC preparation were optimized on the basis of the adsorption efficiency of MB dye (>80%). RM was used as a precursor lignocellulosic material. At first, physical AC was prepared by the carbonization of homogeneous particle size of RM. Thereafter, this physical AC was activated chemically. During the preparation of physical AC, RM was carbonized using the following two steps: (i) heating at 400°C for 1 h under a continuous stream of N_2 gas and (ii) carbonization at 500°C for 90 min under a CO_2 gas stream. Afterwards, for chemical activation the carbonized material (developed in step (i)) was impregnated with 1 M KOH (1:3 ratio) overnight, subsequently washed with deionized water and dried at 90°C for 24 h. Thereafter, the resulting material was impregnated with concentrated H_2SO_4 (1:2 ratio) for 1 h. Then, it was washed again with deionized water and dried at 90°C for 2 h. Finally, the chemical AC material was sieved through 40 mesh size (420 μm) and used for MB dye adsorption in batch mode.

2.3. Batch adsorption experiments

For both adsorbents, the batch experiments were conducted in 100 mL conical flasks. The shaking speed was maintained at 200 rpm in a temperature controlled orbital shaker at 30°C. A measured amount (0.05 g L^{-1}) of adsorbent was added to a 50 mL solution with an initial dye concentration of 50 mg L^{-1}. The equilibrium distribution of dye between the adsorbent (solid phase) and aqueous phase was recorded for 5 h. The effects of environmental and operational variables on adsorption capacity of the RM and RMAC adsorbents were analyzed. These parameters included the pH (3–10), temperature (25°C–50°C), initial adsorbate concentration (25–200 mg L^{-1}), and agitation speed (100–220 rpm). Solutions of 0.1 M HCl and 0.1 M NaOH were used to adjust the pH which was monitored using a pH metre (Model: PHS-25CW, Shanghai). The amount of MB adsorbed (q_e, mg g^{-1}) per unit weight of adsorbent and the adsorption efficiency (q_e, %) of the RM and RMAC adsorbents were calculated using Eqs. (1) and (2), respectively:

$$q_e = \left(\frac{C_0 - C_f}{m}\right)V \tag{1}$$

$$q_e(\%) = \left(\frac{C_0 - C_f}{m}\right)V \times \frac{100}{C_0} \tag{2}$$

where q_e is the equilibrium concentration of the MB dye (mg g^{-1}), C_o and C_f were the initial and final concentrations of the MB dye (mg L^{-1}), respectively, m and V are the mass of adsorbent (g) and the volume of the solution (L), respectively.

2.4. Isotherm, kinetics and thermodynamics studies

The adsorption isotherms of the MB dye onto RM and RMAC adsorbents were investigated by the frequently used models of Langmuir, Freundlich and Dubinin–Radushkevich (D–R). The best fit for MB adsorption data was analyzed by pseudo-first-order and pseudo-second-order kinetic models, and the mechanism of dye adsorption onto the RM and RMAC was investigated. The corresponding correlation coefficients and constants of the model plots were elucidated. A thermodynamic study was conducted to assess the spontaneity of MB adsorption onto RM and RMAC. To observe the structural stability of RM and RMAC, their structural stabilities were examined at the solid–liquid interface through entropy of the system.

2.5. Characterization of adsorbents

2.5.1. Fourier transform infrared spectroscopy

A Fourier transform infrared (FTIR) spectral analysis of RM and RMAC was performed to reveal the possible functional groups that may participate in MB adsorption. The dried adsorbents (before and after dye loading) were converted into KBr pellets, and the FTIR spectra were recorded by an IRPrestige-21 instrument from Shimadzu, Japan.

2.5.2. Scanning electron microscopy and BET analyses

Scanning electron microscopy (SEM) micrographs were taken with a scanning electron microscope (Hitachi S-3000N, Japan), and the morphologies of RM and RMAC were studied before MB dye adsorption and only in RMAC after MB dye loading. The scans of RM and RMAC adsorbents were taken at an acceleration voltage of 5 kV using a secondary electron detector and a 25 mm working distance was maintained. BET analyses of RM and RMAC adsorbents were conducted under the set conditions, i.e., pressure 0.05–0.3 p/p^o, temperature 77.03 K and warm free space of 9.9562 cm^3.

AQ1
AQ2

2.5.3. Determination of point of zero charge

The behaviour of both RM and RMAC adsorbents under acidic or basic solution conditions was studied by determining the pH at point of zero charge (pH_{pzc}; salt addition method) [20]. For this purpose, 0.5 g of RM or RMAC adsorbent was added to 50 mL of 0.1 M NaCl solution in 100 mL conical flasks. The initial pH (pH_i) of the solution (2–10) was adjusted with 0.1 M HCl and 0.1 M NaOH solutions. Both RM and RMAC samples were shaken until the respective equilibrium times of 60 and 180 min in a temperature-controlled orbital shaker at 130 and 200 rpm and 30 and 40°C, respectively. Subsequently, the final pH (pH_f) was measured. The change in pH (ΔpH) was plotted against the pH_i, and then pH_{pzc} was noted when ΔpH = 0.

2.6. Statistical analysis

All the measurements reported in this study are the average values of at least three independent measurements. One-way analysis of variance was performed using Statistica Statsoft Software 10, and the least significant differences of means were reported at $p = 0.01$.

3. Results and discussions

3.1. Effects of different reaction parameters

3.1.1. Effects of the agitation speed

The effects of the agitation speed on the MB dye adsorption efficiency of RM and RMAC are shown in Fig. 1. The adsorption efficiencies of RM and RMAC showed an increasing trend with the agitation speed [24]. This observation is probably due to the decreased thickness of the boundary layer around the RM and RMAC adsorbents, which can be associated with the increased turbulence effect. MB dye adsorption capacity did not significantly increase ($p = 0.01$) after 130 rpm for RM, i.e., 26.28 mg g^{-1} (52.56%) and 200 rpm for RMAC, i.e., 39.81 mg g^{-1} (80%). The adsorption capacity reflected the conclusion that the agitation speed for each adsorbent should be explored. In the current study, further batch experiments were conducted at 130 rpm for RM and 200 rpm for RMAC to study the effects of other process variables. Similar results were also reported by Al-Qodah [25] for the dye's adsorption on shale oil ash.

3.1.2. Effects of contact time

The adsorption capacities of RM and RMAC for MB dyes were studied over a contact time range of 20–300 min, as shown in Fig. 2. The effect of the contact time on adsorption efficiency of RM and RMAC remained significant ($p = 0.01$) until 60 and 180 min, where the maximum adsorption capacity was observed at 23.86 mg g^{-1} (48%) and 39.40 mg g^{-1} (79%), respectively. In the case of both RM and RMAC, MB adsorption occurred in two steps. In the first step, fast MB adsorption occurred in 40 min because of large number of available active sites on the adsorbents. The duration of the moderate second step lasted until the active sites were filled, and equilibrium was established for RM at 60 min and for RMAC at 180 min. Afterwards, there was no significant increase in the MB adsorption capacity of either adsorbent. Therefore, the equilibrium adsorption time for RM and RMAC adsorbents was marked 60 and 180 min, respectively. Further batch studies were carried out at the aforementioned equilibrium times for both types of adsorbents. A similar result for the adsorption of MB was reported by Hameed et al. [26].

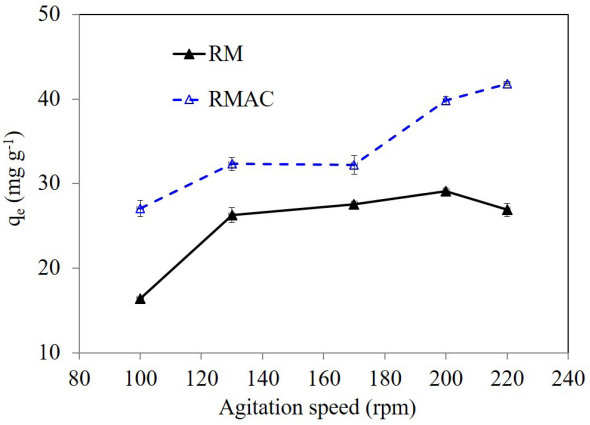

Fig. 1. Effects of agitation speed on the MB dye adsorption capacities of RM and RMAC.

3.1.3. Effects of pH

The maximum MB adsorption capacity of RM, i.e., 18.91 mg g^{-1} (38%), was observed at pH 9 when compared with RMAC, the latter displayed a maximum capacity of 34.52–40.38 mg g^{-1} over a pH range of 3–10 (Fig. 3). The solution pH affected the adsorption of contaminant by playing with surface charges present on the surface of the adsorbents. For the RM adsorbent, increasing the pH from 3 to 7 revealed a slight increase in the adsorption of MB. In acidic environments, this result can be ascribed to the presence of more H ions, which may compete with the MB dye for adsorption to active sites. Adsorption is due to the electrostatic interaction between the positively charged MB molecules and negatively charged RM surface [27]. At a higher solution pH (8–9), negatively charged sites increased in number, and in turn, these sites further increased the adsorption capacity of the adsorbent for cationic dye [28]. However, in the case of RMAC, MB removal efficiency increased significantly (p = 0.01), from 69% at pH 3 to 81% at pH 10. However, there was no significant (p = 0.01) difference between the removal efficiency of the acidic and basic environment, i.e., at pH 4, 6 and 10. Moreover, RMAC displayed a higher MB adsorption efficiency than RM. The results are in agreement with pH_{pzc}. pH_{pzc} is a good indicator of the surface charge as a function of pH. It helps to understand the dye adsorption behaviour by the respective adsorbent. The pH_{pzc} values for RM and RMAC were 6 and 2. These values reflect that MB adsorption is favoured at pH > pH_{pzc}. Because the development of negative changes on both RM and RMAC adsorbents at pH > pH_{pzc} favour the binding of cationic dye through electrostatic attraction The adsorption of MB dye by RM and RMAC is at a maximum pH values higher than 6.0 and 2.0, respectively.

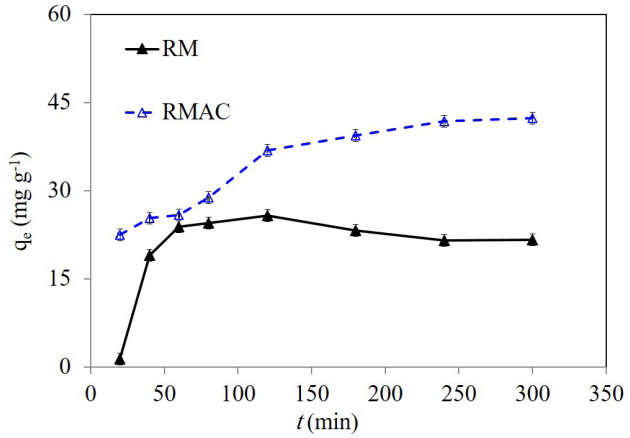

Fig. 2. Effects of contact time on the MB dye adsorption capacities of RM and RMAC.

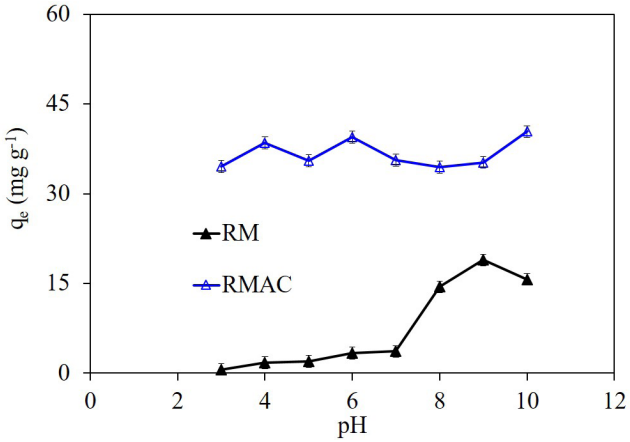

Fig. 3. Effects of pH on the MB dye adsorption capacities of RM and RMAC.

3.1.4. Effects of initial dye concentration

The concentration of the dye provides the driving force to overcome the mass transfer resistance of dye molecules at solid–liquid interfaces. Adsorption capacities of both RM and RMAC adsorbents for MB dye were also examined over variable initial dye concentration ranges of 25–300 mg L^{-1} (Fig. 4). Adsorption of RM and RMAC was significantly high (p = 0.01) at higher concentrations of MB dye, i.e., 71.64 mg g^{-1} (23.88%) and 158.65 mg g^{-1} (52.88%) compared with lower initial concentration, i.e., 9.92 mg g^{-1} (39.69%) and 22.16 mg g^{-1} (88.64%) (Fig. 4). The high adsorption can be associated with high-mass transfer driving force at a high initial MB dye concentration. A lower MB dye adsorption by RMAC at higher concentrations suggests the involvement of chemisorption rather than physical adsorption in the case of the RM adsorbent. Similar results were reported by Senthilkumaar et al. [29] on the adsorption of the MB dye on jute fibre carbon.

3.1.5. Effects of temperature

Fig. 5 shows the effects of temperature on the adsorption capacities of RM and RMAC. RM showed a decrease in MB adsorption in the temperature range of 30°C–40°C, and afterwards, it increased in the range of 40°C–50°C. This trend reflected the exothermic and endothermic behaviour of RM during MB dye adsorption, respectively [30]. On the contrary, RMAC revealed only the endothermic nature during MB dye adsorption because MB dye adsorption increased continuously from 32.91 mg g^{-1} (65%) to 42.61 mg g^{-1} (85%) with increasing temperatures from 30°C to 50°C. Similar results

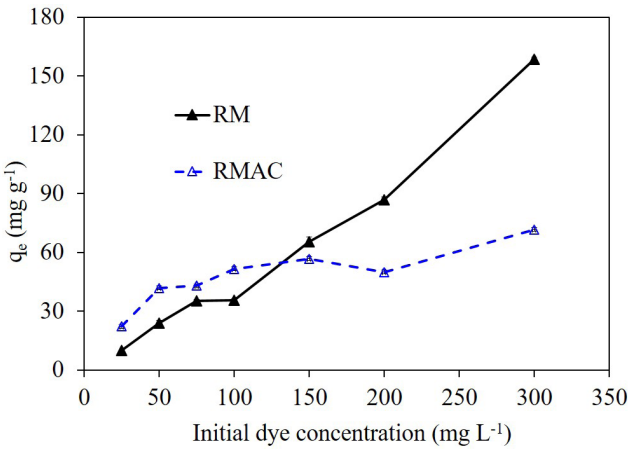

Fig. 4. Effects of initial MB dye concentrations on the MB adsorption capacities of RM and RMAC.

were reported by Zohre et al. [31] for MB dye adsorption onto carbon nanotubes.

3.1.6. MB dye removal by RM and RMAC adsorbents at optimum conditions

The maximum MB adsorption capacities of both RM and RMAC were determined separately as a function of agitation speed, contact time, pH, initial dye concentration and temperature. Thereafter, in second step, the respective conditions of maximum MB adsorption by RM and RMAC were maintained in a single batch experiment, and the optimum MB adsorption capacities were recorded. The maximum adsorption capacity for RM adsorbent was recorded as 153.17 mg g^{-1} at following optimum conditions; an agitation speed of 130 rpm, an equilibrium time of 60 min, a pH of 9, initial dye concentration of 300 mg L^{-1} and a temperature of 30°C. In contrast, RMAC shows the maximum MB dye adsorption of 110.65 mg g^{-1} at the following optimum conditions; an agitation speed of 200 rpm, an equilibrium time of 180 min, a pH of 10, an initial dye concentration of 300 mg L^{-1} and a temperature of 30°C.

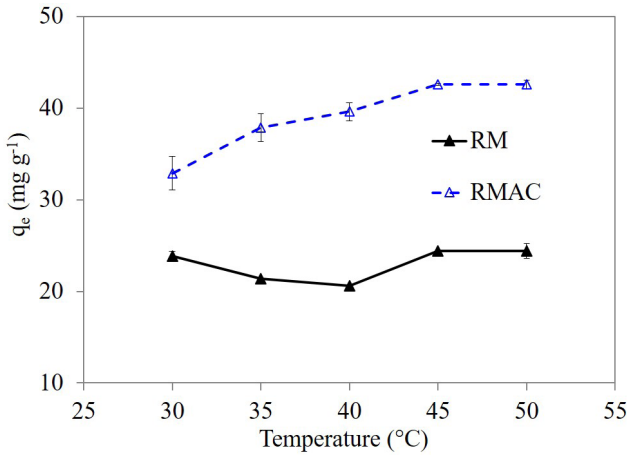

Fig. 5. Effect of temperature on the MB adsorption capacities of RM and RMAC.

3.2. Characterization of RM and RMAC adsorbents

3.2.1. FTIR analyses

Functional groups at the surface of RM adsorbent are analyzed by FTIR before and after MB dye loading (Fig. 6). The following characteristic peaks appeared after analysing the surface of the RM adsorbent before MB adsorption, i.e., 3,356, 2,910, 1,633, 1,361, 1,242 and 1,033 cm^{-1}, which can be ascribed to N–H stretching (amines/amides), C–H stretching (alkanes), N–H bending (amine), C–H bending (alkane) and C–N stretching (aliphatic amine), respectively.

The peak intensities of aliphatic amines were reduced from 1,242 to 1,161 cm^{-1} after MB adsorption. Moreover, alkanes were converted to weak alkynes (from 2,910 to 2,090 cm^{-1}) and aromatic amines (from 1,633 to 1,600 cm^{-1}) after the MB dye adsorption onto RM adsorbent (Fig. 6(a)).

After the conversion of RM adsorbent into AC, i.e., RMAC, peaks were observed from the RMAC surface before MB dye adsorption at 1,593, 1,325, 1,037 and 883 cm^{-1}, which were associated with C–C stretching (aromatic rings), N–O symmetric stretching (nitro compounds), C–N stretching (aliphatic amine) and C–H bending (alkanes), respectively. After MB dye adsorption, some new peaks were formed at 3,350 and 2,885 cm^{-1}, which can be associated with N–H stretching (amines/amides) and C–H stretching (alkanes), respectively [32]. Moreover, some shifts in the FTIR peaks were observed, i.e., from 1,037 to 1,033 cm^{-1}, 1,325 to 1,242 cm^{-1} and 1,593 to 1,597 cm^{-1} (Fig. 6(b)).

3.2.2. SEM analyses

The variation in surface morphology is evident in RM, surface functionalized RMAC and RMAC after MB adsorption (Fig. 7). The SEM images were taken at a magnification

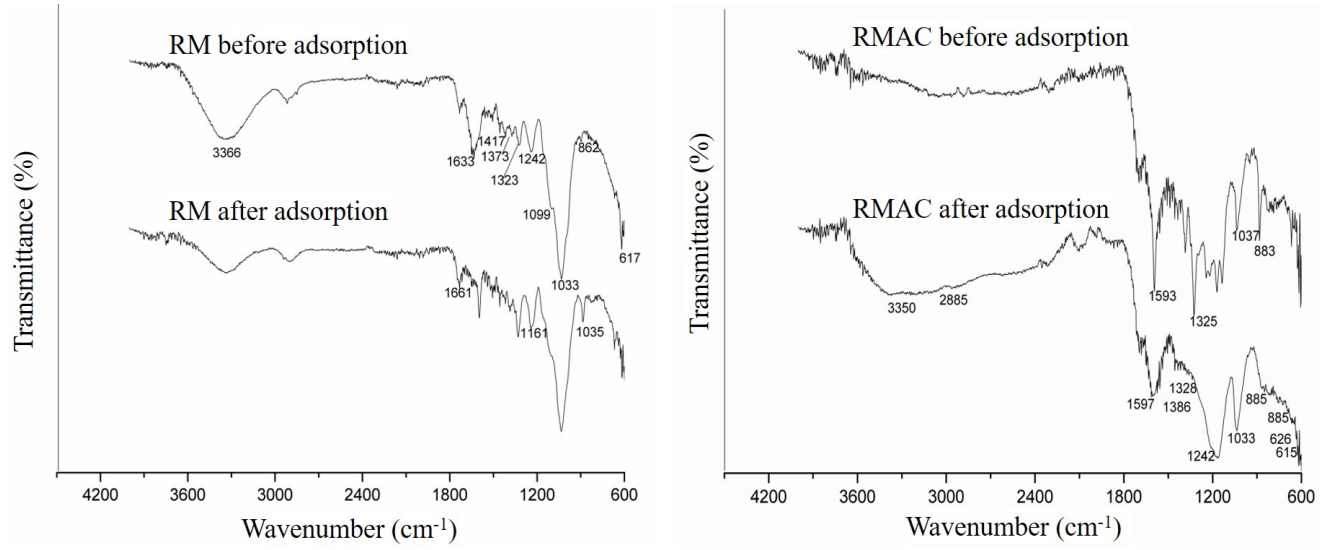

Fig. 6. FTIR analysis of RM (a) and RMAC (b) adsorbent surfaces before and after MB dye adsorption.

of 1,500×. There were only cylindrical structures present with no visible porosity on the surface of the raw RM adsorbent. However, after the physical activation followed by surface functionalization and chemical activation, RMAC displayed large primary pores, and smaller secondary pores were also noticeable inside the primary pores (Fig. 7). These pores on the surface of RMAC can participate in the removal of MB dye. Consequently, the MB removal efficiency of RMAC could be higher than inactivated RM.

3.2.3. BET analyses

According to BET analysis, the surface area of the RM and RMAC were observed as 1.40 and 7.10 $m^2\ g^{-1}$, respectively, with single point adsorption (assuming zero BET intercept). Total pore volume for RM and RMAC were found to be 0.030 and 0.14 $cm^3\ kg^{-1}$, respectively. Both RM and RMAC exhibited the adsorbent average pore width as 2.60 and 7.90 nm, respectively.

3.3. Isotherms and kinetic modelling

Isotherm studies are conducted to correlate the residual concentration (C_e, mg L^{-1}) of adsorbate in the aqueous solution and adsorption capacity (q_e, mg g^{-1}) [33,34]. In this study, various isotherm models, i.e., Langmuir [35], Freundlich [36] and Dubinin–Radushkevich (D–R) [37], were applied to uncover the nature of MB dye adsorption on the surface of RM and RMAC in the solid–liquid equilibrium phase.

3.3.1. Langmuir isotherm

The Langmuir isotherm considers finite adsorption sites on the surface of adsorbents as having equal sizes and shapes, and each vacant site can hold only one molecule of adsorbate in a dynamic equilibrium of adsorbate at the solid–liquid phase. The Langmuir isotherm models, type I and type II, applied in this study can be written using Eqs. (3) and (4), respectively:

$$\frac{1}{q_e} = \frac{1}{K_L.q_{max}C_e} + \frac{1}{q_{max}} \tag{3}$$

$$\frac{C_e}{q_e} = \frac{1}{K_L.q_{max}} + \frac{C_e}{q_{max}} \tag{4}$$

where q_{max} and K_L can be calculated from the slope and intercept of plots of $1/q_e$ vs. $1/C_e$ and C_e/q_e vs. C_e for type I and type II, respectively. C_e (mg L^{-1}) is the equilibrium adsorbate concentration in solution, and q_e (mg g^{-1}) is the equilibrium adsorbent capacity.

Among the studied Langmuir linear models (Table 1), type I proved to be a relatively good fit for the MB adsorption data of the RM adsorbent with a coefficient determination of (R^2) of 0.941. However, the MB adsorption data of RMAC

Table 1
Adsorption isotherm constants

Models		Parameters	RM	RMAC
Langmuir	Type I	q_{exp} (mg g^{-1})	84.52	71.65
		q_{max} (mg g^{-1})	270.27	64.1
		K_L (L mg^{-1})	0.003	0.189
		R_L	0.87	0.19
		R^2	0.941	0.979
	Type II	q_{exp} (mg g^{-1})	–	71.65
		q_{max} (mg g^{-1})	–	51
		K_L (L mg^{-1})	–	0.345
		R_L	–	0.35
		R^2	–	0.998
D–R		q_{DR} (mol g^{-1})	108.55	55.56
		β (mol $J^{-1})^2$	0.008	0.001
		E (kJ mol^{-1})	8.08	28.87
		R^2	0.978	0.975
Freundlich		$1/n$	0.958	0.695
		n	1.04	1.44
		K_F (L g^{-1})	0.87	17
		R^2	0.909	0.993

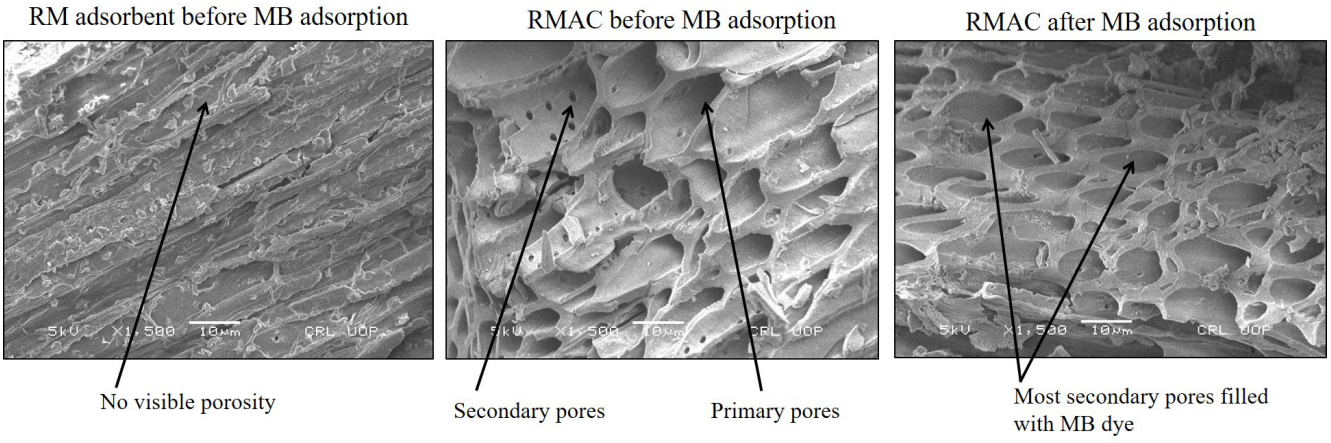

Fig. 7. SEM analyses of RM adsorbent (before) and RMAC adsorbent (before and after) MB dye adsorption.

were shown to be a suitable fit for type II with an R^2 value of 0.998 compared with type I (R^2, 0.979). Langmuir isotherm validity can be explained by equilibrium parameter R_L (separation factor, Eq. (5)) [38], which reveals the suitability of the studied adsorbents for MB dye removal.

$$R_L = \frac{1}{1 + K_L C_0} \tag{5}$$

The adsorption of any pollutant is regarded as favourable if $0 < R_L < 1$, whereas the adsorption is regarded as unfavourable if $R_L > 1$, linear if $R_L = 1$ and irreversible if $R_L = 0$. Although both adsorbents showed favourable MB dye adsorption with R_L values of 0.87 (for RM), 0.19–0.35 (for RMAC), there was a huge difference between q_{exp} and Langmuir q_{max} derived from of the RM data compared with the RMAC data (Table 1). In the latter case, the data reflected the saturation of the adsorbent surface with a monolayer of MB dye molecules.

3.3.2. Dubinin–Radushkevich (D–R) isotherm

This model takes into account the physical and chemical nature of MB dye adsorption with its mean free energy values [39]. This model is shown in Eq. (6):

$$\ln q_e = \ln q_{DR} - \beta\varepsilon^2 \tag{6}$$

where q_{DR} is the theoretical monolayer sorption capacity (mg g^{-1}) and β is the constant of adsorption energy ($mol^2 K J^{-2}$). ε is the Polanyi potential, which is calculated using Eq. (7):

$$\varepsilon = RT \ln\left[1 + \frac{1}{C_e}\right] \tag{7}$$

where R and T are the universal gas constants (8.314 J $mol^{-1} K^{-1}$) and temperature, respectively. The R^2 values of RM (0.978) were observed to be higher than those of Langmuir value reported for the same adsorbent. However, RMAC (0.975) is lower than the Langmuir values of the same adsorbent (Table 1). The theoretical monolayer adsorption capacities (q_{DR}) and the adsorption energy constants (β, $mol^2 J^{-2}$) are determined for RM and RMAC as 108.55 and 55.56 mg g^{-1} and 0.008 and 0.001 $mol^2 J^{-2}$, respectively. The mean free energies (E) needed by one mole of MB dye to reach the adsorption sites from an infinite distance for RM and RMAC are 8.08 and 28.87 kJ mol^{-1}, respectively, and are calculated using Eq. (8).

$$E = \frac{1}{\sqrt{-2\beta}} \tag{8}$$

An E value of approximately 28.87 kJ mol^{-1} is quite large; however, a large E value indicates the chemisorption for the RMAC adsorbent with an ion-exchange mechanism, i.e., 8–16 kJ mol^{-1} [27]. Mechanisms in this range are indicative of strong electrostatic interactions between the negatively charged surface of RMAC and MB dye molecules. However, the E value is reported as 8.08 kJ mol^{-1}, which can be the physical adsorption of MB dye in the case of the RM adsorbent.

3.3.3. Freundlich isotherm

The model described in Eq. (9) assumes the heterogeneous surface of RM and RMAC adsorbents:

$$q_e = K_F c_e^{1/n} \tag{9}$$

where K_F is the relative adsorption and $1/n$ is the heterogeneity factor, both are determined from the q_e vs. C_e plot. These parameters indicate the intensity and adsorption feasibilities, respectively. Exponent values should be <1 for the adsorption process to be favourable [2,36,40]. In this study, these values were determined as 0.867 for RM and 0.695 for RMAC, which revealed the usefulness of the studied adsorbents for MB dye adsorption. However, the Freundlich model proved to be a poor fit to the MB adsorption data of RM than RMAC with R^2 values of 0.909 and 0.993, respectively. Overall, on the basis of R^2, the equilibrium adsorption of MB dye onto RM and RMAC was better described by the Langmuir isotherm than the Freundlich isotherm.

3.3.4. Pseudo-first-order and pseudo-second-order kinetics

The sorption potential of any adsorbent can be assessed as a function of the contact time in that either a contaminant molecule requires a longer or short time for its binding to the adsorbent surface. Adsorption reaction models do not consider the actual mechanism of solute transport; rather, they are based on the whole adsorption process. Because the adsorption rates are sufficient for practical operation point of view. Pseudo-first order (Eq. (10)) is the earliest known rate describing the adsorption rate based on the adsorption capacity:

$$\log(q_e - q_t) = \log q_e - K_1 t / 2.303 \tag{10}$$

where q_t (mg g^{-1}) is the amount of adsorbate adsorbed at time t and K_1 (min^{-1}) is the pseudo-first-order rate constant. The driving force, $(q_e - q_t)$, is proportional to the available fraction of active sites.

For the RM adsorbent, the values of the rate constant (K_1, –0.02 to 0.001 min^{-1}), the calculated adsorption capacity ($q_{e,cal}$, 9.07–14.08 mg g^{-1}) and the correlation coefficients (R^2, 0.4245–0.211) were calculated from $\log(q_e - q_t)$ vs. t plot (Table 2). These following values were observed for the RMAC adsorbent: a K_1 value of –0.021 to 0.013 min^{-1}, a $q_{e,cal}$ value of 11.58–22.12 mg g^{-1} and an R^2 of 0.9337–0.9798. Although the coefficient of regression values for RMAC were high as compared with those exhibited by RM adsorbent at variable initial concentrations of MB dye, these values were not comparable with those of a pseudo-second-order reaction (Table 3). This result indicates that the film diffusion or mass transfer property is not the primary rate controlling process. Moreover, differences between the experimental ($q_{e,exp}$) and calculated ($q_{e,cal}$) q_e demonstrated that the adsorption kinetics of the pseudo-first-order model could not be reproduced. The pseudo-second-order model is based on the assumption of the chemisorption as the rate-limiting step [41].

The model shown in Eq. (11) has the advantage of not having the problem of assigning an effective adsorption capacity, i.e., the adsorption capacity and that the initial adsorption

rate and the constant rate of pseudo-second-order can all be determined from this models without knowing any parameters beforehand.

$$\frac{t}{q_t} = \frac{1}{K_2 q_e^2} + \frac{1}{q_e} t \quad (11)$$

where K_2 (g mg^{-1} min^{-1}) is the pseudo-second-order rate constant and h ($h = K^2 q_e^2$) is the initial adsorption rate (mg g^{-1} min^{-1}), which is a complex function of the solute concentration [42]. These constants were calculated from the intercept and the slope of the plot t/q_t vs. t (Fig. 8). R^2 values were used to determine the validity of the pseudo-second-order kinetic model. The MB adsorption data of both adsorbents seemed to fit the pseudo-second-order kinetic model (Table 3). At lower initial concentrations, the adsorption capacity values of RMAC were closer to those of the experiment than at high initial adsorbate concentrations (Table 3). The suitability of the pseudo-second-order kinetic model to MB adsorption data by RMAC at lower and higher initial dye concentrations reflected the applicability of the RMAC adsorbent with a wide range of contaminant concentrations.

3.4. Thermodynamic study

Thermodynamics parameters were calculated to further observe the effects of temperature on MB adsorption onto RM and RMAC adsorbents (Table 4). The distribution coefficient K_d was calculated from Eq. (12):

Table 2
Pseudo-first-order models for MB adsorption on RM and RMAC adsorbents

Initial MB dye concentration (mg L^{-1})	RM adsorbent				RMAC adsorbent			
	$q_{e,exp}$. (mg g^{-1})	K_1 (min^{-1})	$q_{e,cal}$ (mg g^{-1})	R^2	$q_{e,exp}$. (mg g^{-1})	K_1 (min^{-1})	$q_{e,cal}$ (mg g^{-1})	R^2
30	14.5	–0.02	9.07	0.4245	26.25	–0.021	11.58	0.9337
50	23.86	–0.003	3.22	0.0556	39.40	–0.018	31.20	0.8405
70	41.03	–0.023	16.17	0.5705	41.48	–0.010	23.22	0.8839
90	36.04	–0.001	14.08	0.2114	38.92	–0.013	22.12	0.9798

Table 3
Pseudo-second-order models for MB adsorption onto RM and RMAC adsorbents

Initial MB dye concentration (mg L^{-1})	RM adsorbent					RMAC adsorbent				
	$q_{e,exp}$. (mg g^{-1})	K_2 (g mg^{-1} min^{-1})	$q_{e,cal}$ (mg g^{-1})	h (mg g^{-1} min^{-1})	R^2	$q_{e,exp}$. (mg g^{-1})	K_2 (g mg^{-1} min^{-1})	$q_{e,cal}$ (mg g^{-1})	h (mg g^{-1} min^{-1})	R^2
30	14.5	0.012	10.31	1.24	0.9869	26.25	0.0124	14.03	2.29	0.9984
50	23.86	0.225	12.38	34.48	0.9584	39.40	0.0025	22.99	1.33	0.9688
70	41.03	0.009	22.73	4.76	0.9982	41.48	0.0025	23.37	1.38	0.9604
90	36.04	0.122	12.03	17.73	0.9874	38.92	0.0034	21.79	1.62	0.9938

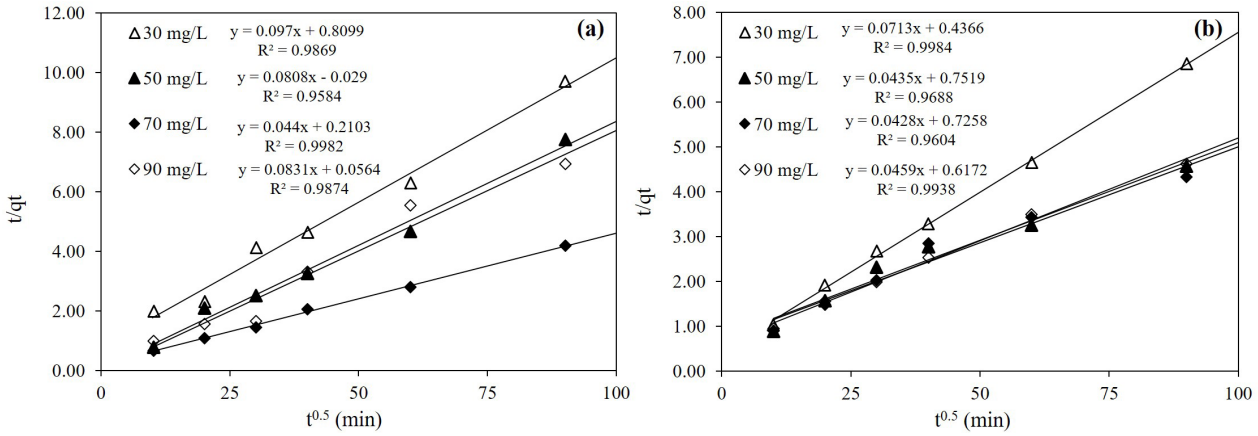

Fig. 8. Pseudo-second-order kinetic plot for MB adsorption onto RM (a) and RMAC (b) adsorbents.

Table 4
Thermodynamic parameters of MB adsorption on RM and RMAC

Adsorbent type	ΔH (kJ mol^{-1})	ΔS (kJ mol^{-1})	ΔG (kJ mol^{-1})				
			303 K	303 K	313 K	318 K	323 K
RM (303–323 K)	–16.35	–0.06	0.34	0.61	0.89	1.17	1.44
RMAC (303–323 K)	43.45	0.15	–1.98	–2.73	–3.48	–4.23	–4.98

$$K_d = \frac{q_e}{C_e} \tag{12}$$

where q_e is the solid phase concentration and C_e is the liquid phase concentration at equilibrium. This equation was further applied to the Van't Hoff plot. Changes in enthalpy and entropy were calculated from the Van't Hoff plot by using Eq. (13):

$$\ln K_d = \frac{\Delta S}{R} - \frac{\Delta H}{\mathrm{RT}} \tag{13}$$

where ΔH (kJ mol^{-1}), ΔS (kJ mol^{-1}) and K_d indicate changes in standard enthalpy, standard entropy and the distribution coefficient (q_e/C_e), respectively. R is a universal gas constant (8.314 J mol^{-1} K^{-1}), and T is the temperature (K). ΔG (Gibbs free energy change, kJ mol^{-1}) values were obtained from Eq. (14).

$$\Delta G = \Delta H - T\Delta S \tag{14}$$

RM and RMAC adsorbents exhibited non-spontaneous (thermodynamically unfavourable) and spontaneous natures of the adsorption process with positive and negative values of Gibbs free energies during MB dye adsorption, respectively. RM displayed an exothermic reaction with negative enthalpy and decreased order at solid–liquid interface (Table 3). For the RMAC adsorbent, the positive values of ΔH and ΔS are 43.45 and 0.15 kJ mol^{-1}, respectively, indicate the endothermic and increased disorder at the solid–liquid interface. Similar observations of endothermic nature have been observed to describe the adsorption process for rhodamine B adsorption by *Aleurites moluccana* seeds [43], remazol brilliant blue R dye adsorption by AC [44], malachite green dye adsorption by spinach leaves [45] and amaranth dye by water hyacinth leaves [46].

4. Conclusions

The adsorption capacities of the RM in its inactive and active forms were investigated in this study for the removal of MB dye under a batch adsorption system. Different reaction parameters affecting the adsorption process were optimized, including the agitation speed, contact time, pH, initial dye concentrations and temperature. Characterization of both adsorbents was performed using the FTIR and SEM analyses. The adsorption mechanisms and adsorptive nature of the RM and RMAC were studied using different isotherm models and reaction kinetics. Finally, the spontaneity of the reaction was assessed through thermodynamic study. The adsorption efficiency of the RMAC for MB dye was almost double (>85%) that of the RM. This result can be attributed to the increased porosity of RMAC after chemical activation. RMAC displayed the maximum MB adsorption efficiency at an equilibrium time of 180 min (79%), an initial dye concentration of 25 mg L^{-1} (89%), a pH of 10 (81%), a temperature of 40°C (80%) and an agitation speed of 200 rpm (80%). The adsorption data of both RM and RMAC were best described by the Langmuir isotherm model, which determined the physical adsorption with a mean free energy of 8.08 kJ mol^{-1}. The Freundlich isotherm model, on the other hand, reflected the chemisorption with a mean free energy of 28.87 kJ mol^{-1}. The fitness of the pseudo-second-order kinetic model using RMAC adsorbent at lower and higher initial dye concentrations reflected its applicability for wide range concentrations of contaminants. The results presented in this study clearly reflect the RMAC adsorbent is more efficient than the RM adsorbent, helping to conclude that RMAC can be used as a superior and more efficient sorbent for MB dye removal in comparison with its non-activated form. It is assumed that RMAC can be used for real wastewater containing dyes, heavy metals, salts and bleaching agents. In order to confirm such assumption, the effect of competition among different contaminants for RMAC adsorption sites on the final removal efficiency shall be investigated using a real wastewater.

Acknowledgement

The project was financially supported by King Saud University, Vice Deanship of Research Chairs.

Conflict of interest

Authors declare no conflict of interest.

References

[1] R. Dod, G. Banerjee, S. Saini, Adsorption of methylene blue using green pea peels (*Pisum sativum*): a cost-effective option for dye-based wastewater treatment, Biotechnol. Bioprocess Eng., 17 (2012) 862–874.
[2] B.H. Hameed, L.H. Chin, S. Rengaraj, Adsorption of 4-chlorophenol onto activated carbon prepared from rattan sawdust, Desalination, 225 (2008) 185–198.
[3] S. Chatterjee, D.S. Lee, M.W. Lee, S.H. Woo, Congo red adsorption from aqueous solutions by using chitosan hydrogel beads impregnated with nonionic or anionic surfactant, Bioresour. Technol., 100 (2009) 3862–3868.
[4] M.F. Abid, M.A. Zablouk, A.M. Abid-Alameer, Experimental study of dye removal from industrial wastewater by membrane technologies of reverse osmosis and nanofiltration, Iran. J. Environ. Health Sci. Eng., 9 (2012) 17.
[5] J.-W. Lee, S.-P. Choi, R. Thiruvenkatachari, W.-G. Shim, H. Moon, Evaluation of the performance of adsorption and coagulation processes for the maximum removal of reactive dyes, Dyes Pigm., 69 (2006) 196–203.

[6] M. Marcucci, G. Nosenzo, G. Capannelli, I. Ciabatti, D. Corrieri, G. Ciardelli, Treatment and reuse of textile effluents based on new ultrafiltration and other membrane technologies, Desalination, 138 (2001) 75–82.
[7] Z. Xue, S. Zhao, Z. Zhao, P. Li, J. Gao, Thermodynamics of dye adsorption on electrochemically exfoliated graphene, J. Mater. Sci., 51 (2016) 4928–4941.
[8] S. Mondal, Methods of dye removal from dye house effluent—an overview, Environ. Eng. Sci., 25 (2008) 383–396.
[9] R. Hoseinzadeh Hesas, W.M.A. Wan Daud, J.N. Sahu, A. Arami-Niya, The effects of a microwave heating method on the production of activated carbon from agricultural waste: a review, J. Anal. Appl. Pyrolysis, 100 (2013) 1–11.
[10] M.J. Prauchner, F. Rodríguez-Reinoso, Chemical versus physical activation of coconut shell: a comparative study, Microporous Mesoporous Mater., 152 (2012) 163–171.
[11] M.M. Ozcan, J.-C. Chalchat, Chemical composition and antifungal activity of rosemary (*Rosmarinus officinalis* L.) oil from Turkey, Int. J. Food Sci. Nutr., 59 (2008) 691–698.
[12] A.K. Genena, H. Hense, A. Smânia Jr., S.M. de Souza, Rosemary (*Rosmarinus officinalis*): a study of the composition, antioxidant and antimicrobial activities of extracts obtained with supercritical carbon dioxide, Food Sci. Technol., 28 (2008) 463–469.
[13] U. Tahir, A. Yasmin, U.H. Khan, Phytoremediation: potential flora for synthetic dyestuff metabolism, J. King Saud Univ. Sci., 28 (2016) 119–130.
[14] Z. Zheng, K. Shetty, Azo dye-mediated regulation of total phenolics and peroxidase activity in thyme (*Thymus vulgaris* L.) and rosemary (*Rosmarinus officinalis* L.) clonal lines, J. Agric. Food Chem., 48 (2000) 932–937.
[15] S. Karthikeyan, C. Amudha, S. Tamilselvi, K. Gopal, Removal of textile dye using carbon nanotubes as an adsorbent in fixed bed column, J. Environ. Nanotechnol., 5 (2016) 17–24.
[16] M. Erhayem, F. Al-Tohami, R. Mohamed, K. Ahmida, Isotherm, kinetic and thermodynamic studies for the sorption of mercury (II) onto activated carbon from *Rosmarinus officinalis* leaves, Am. J. Anal. Chem., 6 (2015) 1–10.
[17] B. Viswanathan, P.I. Neel, T.K. Varadarajan, Methods of Activation and Specific Applications Of Carbon Materials, India, Chennai, 2009.
[18] V. Sricharoenchaikul, C. Pechyen, D. Aht-ong, D. Atong, Preparation and characterization of activated carbon from the pyrolysis of physic nut (*Jatropha curcas* L.) waste, Energy Fuels, 22 (2008) 31–37.
[19] B.N. Thomas, S.C. George, Production of activated carbon from natural sources, Trends Green Chem., (2015).
[20] M. Sharifirad, F. Koohyar, S. Rahmanpour, M. Vahidifar, Preparation of activated carbon from phragmites australis: equilibrium behaviour study, Res. J. Recent Sci., 1 (2012) 10–16.
[21] M. Bilal, J.A. Shah, T. Ashfaq, S.M.H. Gardazi, A.A. Tahir, A. Pervez, H. Haroon, Q. Mahmood, Waste biomass adsorbents for copper removal from industrial wastewater—a review, J. Hazard. Mater., 263, (2013) 322–333.
[22] H. Haroon, T. Ashfaq, S.M.H. Gardazi, T.A. Sherazi, M. Ali, N. Rashid, M. Bilal, Equilibrium kinetic and thermodynamic studies of Cr(VI) adsorption onto a novel adsorbent of *Eucalyptus camaldulensis* waste: batch and column reactors, Korean J. Chem. Eng., 33 (2016) 2898–2907.
[23] M. Amin, A. Alazba, M. Shafiq, Adsorptive removal of reactive black 5 from wastewater using bentonite clay: isotherms, kinetics and thermodynamics, Sustainability, 7 (2015) 15302–15318.
[24] W.-T. Tsai, K.-J. Hsien, H.-C. Hsu, C.-M. Lin, K.-Y. Lin, C.-H. Chiu, Utilization of ground eggshell waste as an adsorbent for the removal of dyes from aqueous solution, Bioresour. Technol., 99 (2008) 1623–1629.
[25] Z. Al-Qodah, Adsorption of dyes using shale oil ash, Water Res., 34 (2000) 4295–4303.
[26] B.H. Hameed, D.K. Mahmoud, A.L. Ahmad, Sorption equilibrium and kinetics of basic dye from aqueous solution using banana stalk waste, J. Hazard. Mater., 158 (2008) 499–506.
[27] K.Y. Foo, B.H. Hameed, Insights into the modeling of adsorption isotherm systems, Chem. Eng. J., 156 (2010) 2–10.
[28] R. Han, Y. Wang, P. Han, J. Shi, J. Yang, Y. Lu, Removal of methylene blue from aqueous solution by chaff in batch mode, J. Hazard. Mater., 137 (2006) 550–557.
[29] S. Senthilkumaar, P.R. Varadarajan, K. Porkodi, C.V. Subbhuraam, Adsorption of methylene blue onto jute fiber carbon: kinetics and equilibrium studies, J. Colloid Interface Sci., 284 (2005) 78–82.
[30] P. Senthil Kumar, P.S.A. Fernando, R.T. Ahmed, R. Srinath, M. Priyadharshini, A.M. Vignesh, A. Thanjiappan, Effect of temperature on the adsorption of methylene blue dye onto sulfuric acid-treated orange peel, Chem. Eng. Commun., 201 (2014) 1526–1547.
[31] S. Zohre, S.G. Ataallah, A. Mehdi, Experimental study of methylene blue adsorption from aqueous solutions onto carbon nano tubes, Int. J. Water Resour. Environ. Eng., 2 (2010) 16–28.
[32] M.H. Mas Haris, K. Sathasivam, The removal of methyl red from aqueous solutions using banana pseudostem fibers, Am. J. Appl. Sci., 6 (2009) 1690–1700.
[33] M. Auta, B.H. Hameed, Acid modified local clay beads as effective low-cost adsorbent for dynamic adsorption of methylene blue, J. Ind. Eng. Chem., 19 (2013) 1153–1161.
[34] M.S.U. Rehman, I. Kim, J.-I. Han, Adsorption of methylene blue dye from aqueous solution by sugar extracted spent rice biomass, Carbohydr. Polym., 90 (2012) 1314–1322.
[35] I. Langmuir, The adsorption of gases on plane surfaces of glass, mica and platinum, J. Am. Chem. Soc., 40 (1918) 1361–1403.
[36] H. Freundlich, Over the adsorption in solution, J. Phys. Chem., 57 (1906) 385–471.
[37] M.M. Dubinin, L.V. Radushkevich, Equation of the characteristic curve of activated charcoal, proceedings of the academy of sciences, Phys. Chem. Sect. USSR, 55 (1947) 331–333.
[38] K.R. Hall, L.C. Eagleton, A. Acrivos, T. Vermeulen, Pore- and solid-diffusion kinetics in fixed-bed adsorption under constant-pattern conditions, Ind. Eng. Chem. Fundam., 5 (1966) 212–223.
[39] M.M. Dubinin, The potential theory of adsorption of gases and vapors for adsorbents with energetically nonuniform surfaces, Chem. Rev., 60 (1960) 235–241.
[40] M. Ahmaruzzaman, S.L. Gayatri, Activated tea waste as a potential low-cost adsorbent for the removal of *p*-nitrophenol from wastewater, J. Chem. Eng. Data, 55 (2010) 4614–4623.
[41] B.H. Hameed, M.I. El-Khaiary, Batch removal of malachite green from aqueous solutions by adsorption on oil palm trunk fibre: equilibrium isotherms and kinetic studies, J. Hazard. Mater., 154 (2008) 237–244.
[42] N.A. Oladoja, C.O. Aboluwoye, Y.B. Oladimeji, A.O. Ashogbon, I.O. Otemuyiwa, Studies on castor seed shell as a sorbent in basic dye contaminated wastewater remediation, Desalination, 227 (2008) 190–203.
[43] D.L. Postai, C.A. Demarchi, F. Zanatta, D.C.C. Melo, C.A. Rodrigues, Adsorption of rhodamine B and methylene blue dyes using waste of seeds of *Aleurites moluccana*, a low cost adsorbent, Alexandria Eng. J., 55 (2016) 1713–1723.
[44] M.A. Ahmad, S.G. Herawan, A.A. Yusof, Equilibrium, kinetics, and thermodynamics of remazol brilliant blue r dye adsorption onto activated carbon prepared from pinang frond, ISRN Mech. Eng., 2014 (2014) e184265.
[45] O.M. Atoyebi, O.S. Bello, Indian spinach leaf powder as adsorbent for malachite green dye removal from aqueous solution, Covenant J. Phys. Life Sci., 2 (2014).
[46] I. Guerrero-Coronilla, L. Morales-Barrera, E. Cristiani-Urbina, Kinetic, isotherm and thermodynamic studies of amaranth dye biosorption from aqueous solution onto water hyacinth leaves, J. Environ. Manage., 152 (2015) 99–108.

AQ3 AQ4 AQ5